



A DOTA based bisphosphonate with an albumin binding moiety for delayed body clearance for bone targeting☆



Marian Meckel ^a, Vojtěch Kubíček ^b, Petr Hermann ^b, Matthias Miederer ^c, Frank Rösch ^{a,*}

^a Institute of Nuclear Chemistry, Johannes-Gutenberg-University Mainz, Germany

^b Department of Inorganic Chemistry, Charles University, Prague, Czech Republic

^c Department of Nuclear Medicine, University Hospital, Mainz, Germany

ARTICLE INFO

Article history:

Received 1 May 2016

Received in revised form 19 June 2016

Accepted 25 July 2016

Keywords:

Bisphosphonate

PET

Bone metastases

⁶⁸Ga

Albumin-binder

DOTA

ABSTRACT

Radiolabeled bisphosphonates are commonly used in the diagnosis and therapy of bone metastases. Blood clearance of bisphosphonates is usually fast and only 30%–50% of the injected activity is retained in the skeleton, while most of the activity is excreted by the urinary tract. A longer blood circulation may enhance accumulation of bisphosphonate compounds in bone metastases. Therefore, a chemically modified macrocyclic bisphosphonate derivative with an additional human albumin binding entity was synthesized and pharmacokinetics of its complex was evaluated. The DOTA-bisphosphonate conjugate BPAMD was compared against the novel DOTAGA-derived albumin-binding bisphosphonate DOTAGA(428-D-Lys)M^{BP} (L1). The ligands were labeled with ⁶⁸Ga(III) and were evaluated in *in vitro* binding studies to hydroxyapatite (HA) as well as to human serum albumin. The compounds were finally compared in *in vivo* PET and *ex vivo* organ distribution studies in small animals over 6 h. Binding studies revealed a consistent affinity of both bisphosphonate tracers to HA. Small animal PET and *ex vivo* organ distribution studies showed longer blood retention of [⁶⁸Ga]L1. [⁶⁸Ga]BPAMD is initially more efficiently bound to the bone but skeletal accumulation of the modified compound and [⁶⁸Ga]BPAMD equalized at 6 h p.i. Ratios of femur epiphyseal plate to ordinary bone showed to be more favorable for [⁶⁸Ga]L1 than for [⁶⁸Ga]BPAMD due to the longer circulation time of the new tracer. Thus, the chemical modification of BPAMD toward an albumin-binding bisphosphonate, L1, resulted in a novel PET tracer which conserves advantages of both functional groups within one and the same molecule. The properties of this new diagnostic tracer are expected to be preserved in ¹⁷⁷Lu therapeutic agent with the same ligand (a theranostic pair).

© 2016 Elsevier Inc. All rights reserved.

1. Introduction

The bone is frequently affected by metastatic invasion of tumor cells as a consequence of various cancer diseases. This is also accompanied by several symptoms like severe pain, spinal cord compression and hypercalcemia. Tumor cell invasion into the skeleton causes an activation of the osteoclasts and osteoblasts. They liberate signal molecules resulting in a feedback mechanism which is called the *vicious cycle* [1]. Common treatments include chemotherapy, analgesic medication, hormone or bisphosphonate treatments, and external radiation therapy.

Another therapeutic option is utilization of bone-seeking radiopharmaceuticals and they showed good results in the palliative care in the last decades [2,3]. The early approved β^- emitters [³²P]PO₄³⁻ and ⁸⁹SrCl₂ are now replaced by radiotracers carrying radionuclides emitting

particles with lower β^- energy as [¹⁵³Sm]EDTMP and [¹⁷⁷Lu]EDTMP (Chart 1) which cause less side effects to the radiosensitive bone marrow. Recently approved α -particle emitting ²²³RaCl₂ showed, beside pain relief, an overall longer survival rate of three months in prostate cancer patients afflicted by bone metastases [4]. Several more rather experimental compounds and nuclides have appeared as, e.g., [¹⁸⁶Re]HEDP, [^{117m}Sn]DTPA, or macrocyclic DOTA-bisphosphonate conjugates as [⁹⁰Y]DOTA-HBP [5,6]. One of these new compounds is BPAMD (Chart 1), a simple DOTA-bisphosphonate conjugate whose complexes have been proven to effectively seek bone tissue [7]. In contrast to the open-chain chelating agents such as HEDP and EDTMP (Chart 1), the macrocyclic tetraazaligands are able to complex the positron emitting PET radionuclide ⁶⁸Ga(III) as well as the therapeutic low-energy β^- emitter ¹⁷⁷Lu(III) [8]. The ⁶⁸Ga-BPAMD or ¹⁷⁷Lu-BPAMD complexes showed a high and stable bone accumulation associated with a fast pharmacokinetic [9]. ⁶⁸Ga-BPAMD was shown to image bone metastases very well in rat tumor model [10,11]. First ⁶⁸Ga PET scan of human patient [12] proved the high potential of this tracer as a useful theranostic agent enabling utilization of ⁶⁸Ga/¹⁷⁷Lu theranostic pair for the detection and treatment of skeletal metastases [13]. ¹⁷⁷Lu-BPAMD is now becoming more widely used

☆ This is a free access article and can also be viewed on the journal's Web site (www.nucmedbio.com). Complimentary access to this article is available until the next issue publishes online.

* Corresponding author at: Institute of Nuclear Chemistry, University of Mainz, Fritz-Strassmann-Weg 2, D-55126, Mainz, Germany.

both in experimental preclinical work [14,15] and in patients for treatment of bone metastases [16] and a kit for its possible regular production in hospitals has been developed [17].

In previous small animal studies, it was shown that radiolabeled bisphosphonates such as ^{68}Ga -BPAMD and ^{177}Lu -BPAMD have a fast blood clearance and almost half of the injected dose is excreted via the kidneys [10,11]. Generally, only 30%–40% of the injected dose remained exclusively on the bone. Most of the activity was washed out of the body via the urinary system [18][9–11] and, therefore, it is no longer available for a binding on the target calcified tissue. In order to delay that fast elimination we investigated a strategy similar to that used for gadolinium(III)-containing MRI contrast agents. To extend blood retention, those compounds were modified with an albumin-binding moiety. The approach has been widely used in development of MRI contrast agents where gadolinium(III) complexes with polydentate aminocarboxylate ligands are applied [19]. Dumelin et al. [20] tested several albumin-binding moieties in conjugation with MRI and fluorescence agents. A simple and available albumin-binding moiety, a *p*-iodophenylbutyric acid residue, induced a relative strong binding ($K_d = 3.3 \mu\text{M}$) of Gd(III)-DTPA to human serum proteins and the complex blood half-life was shifted from $t_{1/2,\alpha} = 8.3 \text{ min}$ for Gd-DTPA to $t_{1/2,\alpha} = 22.3 \text{ min}$ for the Gd-DTPA-albumin-binder derivative. Furthermore, it has been reported that [$^{67/68}\text{Ga}$]DOTA-folate conjugates show an unfavorable tumor-to-kidney ratio due to expression of folate receptors in the kidneys as well as in the targeted folate-positive tumor tissue. Here again, the ratio was improved by utilization of an albumin-binding tracer [21]. Müller et al. [22] further developed the concept of the albumin-binding DOTA-folate conjugate to improve a ^{177}Lu -endoradiotherapy with a folate agent having an enhanced tumor-to-kidney ratio. The same strategy was successfully adapted for a new ^{18}F -labeled folate conjugated with an albumin binder where kidney uptake was reduced to a quarter compared to analogous previously published folate receptor targeting compounds [23]. The longer blood circulation time of these new conjugates resulted in distinctly higher accumulation of such tracers in the target tissue.

Since radiolabeled bisphosphonate-based bone tracers have a fast body clearance, a longer blood retention could (i) minimize unintended urinary exertion, (ii) keep the compound within the blood pool compartment for a longer period of time and (iii) consequently enhance the uptake of the compound on the targeted bone tissue. In addition, a better metastases-to-bone ratio might be achieved. Furthermore, longer blood retention of radiolabeled bisphosphonate conjugates may have the same therapeutic effect with a reduced administered dose, if compared to radiolabeled common bisphosphonates where almost half of the injected dose is excreted within a few minutes. To evaluate the possibility of higher bone delivery of radiolabeled bisphosphonates caused by albumin binding, we synthesized an albumin-binding DOTA-bisphosphonate conjugate DOTAGA(428-D-Lys) M^{BP} (L1, Chart 1). The compound was labeled with ^{68}Ga (III) and properties of this PET tracer were compared to [^{68}Ga]BPAMD in *in vitro* essays, in *in vivo* small animal PET and in *ex vivo* biodistribution studies.

2. Materials and methods

2.1. General

Starting materials, *t*Bu₂-*trans*-DO2A (**1**) [24], 1-*t*-butyl-5-benzyl ester of α -bromoglutaric acid (**2**) [25], and tetraethyl chloro-acetamidomethylbis(phosphonate) (**4**) [7], and BPAMD [7] were synthesized by published methods. All chemicals and solvents were commercially available in analytical, HPLC or TraceSELECT[®] grade and were purchased from Sigma-Aldrich or Merck KgaA. ^{68}Ga was obtained from a $^{68}\text{Ge}/^{68}\text{Ga}$ Obninsk generator system (Eckert & Ziegler). Nuclear magnetic resonance spectra (NMR) were recorded on a Bruker 300 (^1H) or a Bruker 600 (^{31}P) instrument. Mass spectra were recorded on Agilent Technologies 6130 Quadrupole LC/MS spectrometer with ESI as ion source in positive or negative modes. TLC and radio-TLC analyses were carried out on silica on aluminium foil (Merck KgaA) and a Canberra Packard Instant Imager as a radiodetector. For HPLC and radio-HPLC, a Waters-system 1525 with an UV- and a radio-detectors (Berthold Technologies, Germany) was used. Radioactivity of samples was measured with an Aktivimeter Isomed 2010, MED (Nuklear-Medizintechnik Dresden GmbH). Radioactivity in tissue samples was determined by using a Wallac WIZARD2 automatic gamma counter (PerkinElmer, Germany).

2.2. Synthesis of DOTAGA(428-D-Lys) M^{BP} (L1)

2.2.1. Synthesis of **3**

To a solution of **2** (0.6 mg, 1.69 mmol) in dichloromethane (1 mL), a solution of **1** (1.0 g, 2.5 mmol) in dichloromethane (3 mL) was added slowly under vigorous stirring. The mixture was kept at room temperature for 48 h. Volatiles were removed under reduced pressure and the crude mixture was purified by column chromatography utilized on silica (CH_2Cl_2 :MeOH 10:1). The fraction containing the pure product was evaporated to yield **3** as a yellow solid (0.85 mg, 1.25 mmol, 74%). R_f (silica, CH_2Cl_2 :MeOH 10:1) = 0.6–0.7. $^1\text{H-NMR}$ (CDCl_3 , 300 MHz): δ 7.30–7.41 (m, 5H, aryl-H), 5.10 (s, 2H, benzyl- CH_2 -O), 3.40 (t, 1H, N-*CH*-glut.), 3.24–3.36 (m, 4H, N- CH_2 -CO), 2.68–3.04 (m, 16H, cyclen- CH_2 -N), 2.46–2.54 (m, 2H, CH_2 - CH_2 -CO), 1.88–2.04 (m, 2H, CH_2 - CH_2 -CH), 1.43 (s, 27H, *t*Bu). ESI-MS(+): calcd. 676.9, obsd. 678 ($\text{M} + \text{H}^+$), 339.5 ($\text{M} + 2\text{H}^+$).

2.2.2. Synthesis of **5**

Compound **3** (304 mg, 0.45 mmol) was dissolved in dry acetonitrile (5 mL), potassium carbonate (1.3 mmol) was added and compound **4** (255 mg, 0.67 mmol, 1.5 equiv.) was added dropwise to the suspension over a period of 1 h. The reaction mixture was stirred at 40 °C for 24 h. Charcoal was added and all solids were removed by filtration. Volatiles were evaporated and the resulting oil was purified by column chromatography on silica (CHCl_3 :MeOH 10:1) yielding the product as a yellow oil (234 mg, 0.23 mmol, 51%). R_f (silica, CHCl_3 :MeOH 10:1) = 0.3–0.4. $^1\text{H-NMR}$ (CDCl_3 , 300 MHz): δ 7.31–7.44 (m, 5H, aryl-H), 5.11 (s, 2H, benzyl- CH_2 -O), 4.09–4.42 (m, 8H, O- CH_2 - CH_3 ; m, 1H, P-*CH*-P),

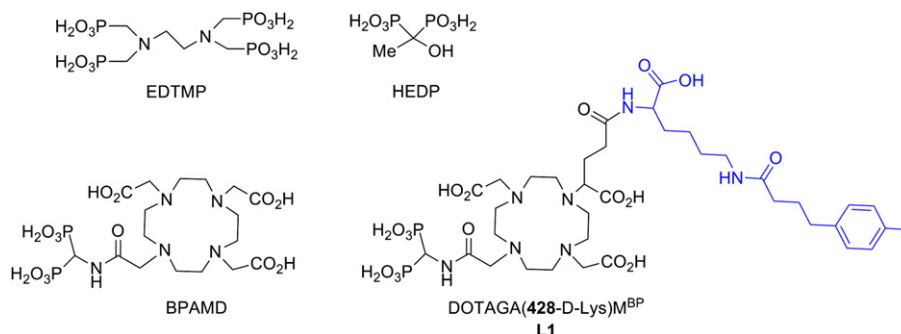


Chart 1. Structure of ligands discussed in this paper.

3.67–3.78 (q, 1H, N-CH-glut.), 3.49 (bs, 6H, N-CH₂-CO), 2.01–3.02 (bm, 20H), 1.46 (s, 27H, tBu), 1.35 (t, 12H, CH₂-CH₃). ESI-MS(+): calcd. 1019.5, obsd. 1020 (M + H⁺), 510 (M + 2H⁺).

2.2.3. Synthesis of **6**

Compound **5** (234 mg, 0.23 mmol) was dissolved in methanol (10 mL) and 10% (w/w) Pd/C (25 mg) was added. The mixture was kept under hydrogen atmosphere (6 bar) in a pressured vessel for 24 h. The solids were removed by filtration over celite and volatiles were evaporated to dryness. The crude product (217.6 mg, 96%) was used in the next step without any further purification. The acidic form of compound **5** was dissolved in dry dichloromethane (5 mL) and HATU (72.3 mg, 0.2 mmol) and *N,N*-diisopropylethylamine (DIPEA, 65 mg, 0.5 mmol) were added. The mixture was stirred at room temperature until all solids were dissolved. Subsequently, *H*-D-Lys(Z)-OMe (63.85 mg, 0.19 mmol) was added in small portions, and the solution was stirred overnight. The reaction mixture was diluted up to 25 mL with dichloromethane and washed always three times with a 0.1 M aq. Na₂CO₃ (25 mL), 0.1 M aq. NaH₂PO₄ (25 mL) and finally with water (25 mL). The organic phase was evaporated to dryness and the crude product was purified by column chromatography on silica (CHCl₃:MeOH 10:1). The fractions containing pure product were combined and evaporated to give a yellow oil (180.6 mg, 0.15 mmol, 65%). *R*_f (silica, CHCl₃:MeOH 10:1) = 0.2–0.3. ¹H-NMR (CDCl₃, 300 MHz): δ 7.32–7.40 (m, 5H, aryl-*H*), 5.10 (s, 2H, benzyl-CH₂-O), 4.41–4.51 (m, 1H, P-CH-P) 4.07–4.33 (m, 8H, O-CH₂-CH₃), 3.73 (bs, 6H, N-CH₂-CO), 1.64–3.69 (bm, 30H, N-CH-glut, cyclen-*H*, glut-*H*, lys-*H*), 1.47 (s, 27H, tBu), 1.36 (t, 12H, CH₂-CH₃). ESI-MS(+): calcd. 1206.34, obsd. 603.8 (M + 2H⁺).

2.2.4. Synthesis of **7**

Compound **6** (180.6 mg, 0.15 mmol) was dissolved in methanol, 10% (w/w) Pd/C was added and the solution was kept under hydrogen atmosphere (5 bar) for 12 h. The solids were filtered off and the solvent was removed to get colorless oil (151.4 mg, 95%) which was used without further purification. 4-(*p*-Iodophenyl)butyric acid (48.7 mg, 0.17 mmol) was dissolved in dry *N*-methyl-2-pyrrolidone (NMP, 2 mL) together with HATU (63.9 mg, 0.17 mmol) and DIPEA (54.26 mg, 0.45 mmol). The mixture was left at room temperature for 15 min and was added to the NMP solution (2 mL) containing the amine obtained from compound **6**. The reaction mixture was stirred overnight and the solvents were removed in vacuum. The crude residue was dissolved in dichloromethane (20 mL) and washed successively always three times with a 0.1 aq. M Na₂CO₃ (20 mL), 0.1 M aq. NaH₂PO₄ (20 mL) and, finally, with water (20 mL). After column chromatography on silica (CHCl₃:MeOH 20:1), a pale foam was obtained (147.8 mg, 0.11 mmol, 73%). *R*_f (silica, CHCl₃:MeOH 20:1) = 0.3–0.4. ESI-MS(+): calcd. 1343.57 obsd. 672.8 (M + 2H⁺).

2.2.5. Synthesis of DOTAGA(428-D-Lys)^{M^{BP}} (L1)

The product was obtained by successive dealkylation of compound **7**. The ester **7** (147.8 mg, 0.11 mmol) was dissolved in a mixture of CH₂Cl₂/TFA 2:3 (50 mL) and the mixture was stirred at room temperature for 12 h. Volatiles were evaporated to dryness and any remaining TFA was removed by repeated co-evaporation with MeOH. Subsequently, the colorless solid was dissolved in dry DMF (2 mL) and trimethylsilyl bromide (TMS-Br, 340 mg, 20 equiv.) was added under argon atmosphere. The reaction mixture was kept at room temperature and by exclusion of light for 12 h. Volatiles were removed under reduced pressure. The TMS-ester was hydrolyzed by dissolving the crude red oil in MeOH. After 12 h, the mixture was evaporated to dryness to yield the crude product (101.2 mg, 85%) which was further purified by semi-preparative reversed-phase HPLC (Hydrosphere C-18, 5-μ, 250 × 10 mm, YMC, Japan) by using a solvent gradient (5 mL/min) of 100% water to 80% acetonitrile within 20 min (*R*_t (L1) = 14.4–15.8 min). Fractions containing the product were determined by ESI-MS(-) and were combined. After lyophilization, a white

solid was obtained (80 mg, 69%). ¹H-NMR (D₂O/NaOD, 300 MHz): δ 7.63 (d, 2H, aryl-*H*, *J*_H = 8.2 Hz), 7.02 (d, 2H, aryl-*H*, *J*_H = 8.2 Hz), 3.33 (bs, 6H, N-CH₂-CO), 3.19 (t, 2H, alkyl-*H*), 2.60 (t, 2H, alkyl-*H*) 1.2–2.6 (bm, 32H, cyclen-*H*, alkyl-*H*). ³¹P-NMR (D₂O/NaOD, 162.05 MHz): δ 14.87 ESI-MS(-): calcd. 1049.24, obsd. 524 (M - 2H⁺).

2.3. Radiolabeling with non-carrier-added (n.c.a.) ⁶⁸Ga and quality control

Ligand L1 (50 μg, 48 nmol) was dissolved in 0.5 M aq. sodium acetate buffer (500 μL; pH = 4) and the solution was added to n.c.a. ⁶⁸Ga (300–600 MBq) which was obtained in a fraction of 400 μL of acetone/HCl obtained from a ⁶⁸Ge/⁶⁸Ga generator system following cationic post-processing [18]. The solution was shaken on a thermoshaker at 98 °C for 15 min. Subsequently, the solution was diluted with deionized water up to 2 mL and passed over a SPE cartridge (Strata X, Phenomenex). The solid phase was first washed with water (3 mL) followed by the elution of the purified product with EtOH/water mixture (1:1, 1 mL). Aliquot samples were taken for radio-HPLC (Hydrosphere C-18, 5-μ, 250 × 10 mm, YMC, Japan, 5 mL/min. Solvent A: of 100% water to 80% acetonitrile within 20 min, (*R*_t (⁶⁸Ga-L1) = 14.9 min) and TLC (silica, solvent: 0.1 M aq. citrate buffer, pH = 4) analyses.

⁶⁸Ga-BPAMD was prepared by dissolving BPAMD (20 μg, 33 nmol) in 0.5 M aq. sodium acetate buffer (500 μL, pH = 4). N.c.a. ⁶⁸Ga solution (400 μL) was added and the reaction mixture was kept on a thermoshaker at 98 °C for 15 min. The solution was diluted with water up to 5 mL and passed over a SPE cartridge (Isolute NH2, Biotage). The cartridge was washed with water (1 mL) followed by the elution of the purified [⁶⁸Ga]BPAMD with phosphate buffered saline (PBS, 2 mL, pH 7.4). Aliquot samples were taken for radio-HPLC (MultoKrom 100 C18, 5-μ, 250 × 4 mm, CS-Chromatographie, Germany, solvent A: 10 mM aq. tetrabutylammonium citrate pH = 4.5, B: ACN, 1 mL/min gradient, 70%(A):30%(B) to 20%(A):80%(B) within 15 min, *R*_t (⁶⁸Ga-BPAMD) = 6.5 min) and TLC (silica, solvent: acetone/acetylacetone/conc. HCl, 10:10:1).

2.4. Adsorption experiments on hydroxyapatite

Hydroxyapatite powder (HA, 20 mg, Sigma-Aldrich) was incubated with isotonic saline (1 mL) for 24 h. The ⁶⁸Ga-labeled bisphosphonate solution (50 μL, prepared as described above) was added and the mixture was vortexed for 15 s. After 10 min standing, the HA was centrifuged at 10×g and the supernatant was removed. Isotonic saline (0.5 mL) was added to the HA fraction, and the vial was vortexed for 15 s and centrifuged again as above. The supernatant was removed and combined with the first solution. Radioactivity was determined in the combined supernatants and the ⁶⁸Ga-complex binding to HA was calculated as percent of ⁶⁸Ga absorbed to HA [8].

2.5. Protein binding assay

Binding of ⁶⁸Ga-BPAMD and [⁶⁸Ga]L1 to serum proteins was determined by ultrafiltration. Each radiotracer solution (50 μL) was added to human serum sample (200 μL, Sigma-Aldrich), the mixture was vortexed and incubated for 1 min. The sample was transferred to a centrifugal device (Nanosep®, 30 K, Pall Corporation, USA) containing a filtration membrane which separates proteins from small molecules. As a control, the radio tracers were incubated in isotonic saline. The ultrafiltration device was centrifuged for 45 min, then isotonic saline (50 μL) was added to wash the filter in an additional 15 min centrifugation step. Radioactivity was counted in the filter and in the filtrate solution, and was calculated as a fraction of the total activity which was set to 100% [13]. The absolute serum binding was calculated as [absolute binding] = [filter activity in human serum] - [filter activity in 0.9% NaCl].

2.6. Animal studies

The experimental procedure used conforms to the European Convention for the Protection of Vertebrate Animals used for Experimental and other Scientific Purposes (ETS No. 123), and to the Deutsches Tierschutzgesetz (German animal welfare regulations). Male Wistar rats (154 ± 24 g, $N = 10$, 1 h; 215 ± 18 g, $N = 12$, 3 h; 220 ± 20 g, $N = 6$, 6 h) were purchased from Charles River Laboratories International, Inc. For dynamic *in vivo* μ PET studies, the animal was anesthetized with isoflurane and placed in supine position in the PET scanner (Siemens microPET, Focus 120). An infrared lamp was used to maintain body temperature. 19.8 MBq ^{68}Ga -BPAMD (107 MBq per kg body weight) and 17.0 MBq ^{68}Ga -L1 (92 MBq per kg body weight) in isotonic saline (0.5 mL) were administered intravenously using a needle catheter into the tail vein. The focus of the μ PET scanner was adjusted to the thorax region. Each compound was tested in one and the same animal within two days. In an additional experiment, the focus of the μ PET scanner was adjusted to the pelvis region to examine the tracer accumulation in the articulation between the femur and the tibia. The investigation was carried out in the same animal within two days. ^{68}Ga -BPAMD (16.3 MBq, 80 MBq per kg body weight) and ^{68}Ga -L1 (16.1 MBq, 79 MBq per kg body weight) in isotonic saline (0.5 mL) were administered intravenously. All images were reconstructed to OSEM2D and processed using Pmod (Pmod Technologies Ltd.) software.

Ex vivo organ distribution was carried out in five animals (male Wistar rats, 160–210 g) per time point. A mean dose of 10 ± 2 MBq of the ^{68}Ga -labeled bisphosphonates in isotonic saline (0.5 mL) was injected intravenously into the tail vein. Animals were sacrificed at 1 h, 3 h and 6 h after injection. The organs of interest were excised and weighed, and the radioactivity in the samples was measured decay- and background-corrected on an automated gamma counter. The activity in the skeleton was calculated by using the activity concentration in the femur and the total skeleton weight (calculated as: skeleton weight (g) = $9.66 + 0.0355 \times \text{BW (g)}$) [10]. Blood density was set to 1.05 mg/mL. The blood volumes (BV) of the Wistar rats were calculated using the formula: $\text{BV (mL)} = 0.06 \times \text{BW (g)} + 0.77$ to determine total blood activities of the radiotracers [26].

2.7. Statistical analysis

All data were expressed as mean \pm standard deviation (SD). Groups were compared using the *t* test. All statistical tests were two tailed, with a *P*-value of less than 0.05 representative for significance.

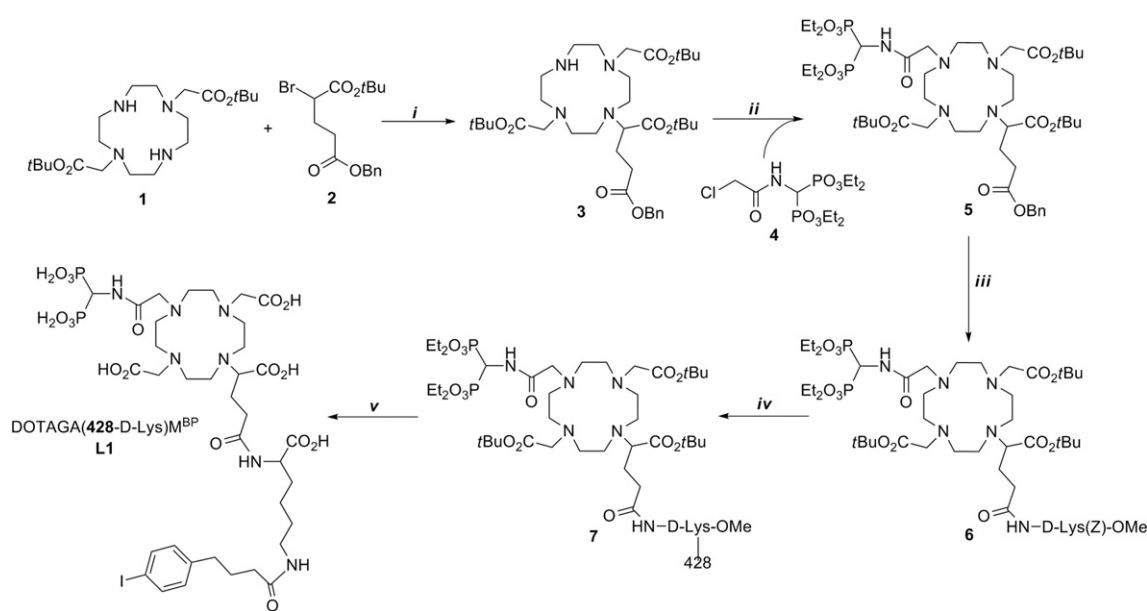
3. Results

3.1. Synthesis (Scheme 1)

Trisubstituted cyclen derivative **3** was formed in reaction of *t*Bu₂-*trans*-DO2A (**1**) [23] with the orthogonally ester protected α -bromoglutaric acid (**2**) [24]. Excess of the macrocyclic nucleophile has to be used to prevent the formation of dialkylated side product. The bisphosphonate-containing pendant arm was introduced by reaction of **3** and chloroacetamide derivative **4** under similar conditions as described for the synthesis of BPAMD [7]. The benzyl ester of **5** was deprotected under standard conditions by hydrogenation. The carboxylic group was activated with HATU and reacted with the orthogonally protected lysine derivative H-D-Lys(Z)-OMe to give compound **6**. The primary amino group in **6** was deprotected by hydrogenation and its reaction with HATU activated 4-(*p*-iodophenyl)butyric acid produced compound **7**. Global ester removal was carried out in two steps. The *t*-butylester group removal by trifluoroacetic acid was followed by *P*-ethyl- and carboxylic methylester deprotection with trimethylsilylbromide (TMS-Br). The desired albumin-binding compound DOTAGA(428-D-Lys)M^{BP} (L1) was finally purified on semi-preparative HPLC (Scheme 1).

3.2. Radiolabeling with *n.c.a.* ^{68}Ga and quality control

Radiochemical yields (RCY) of [^{68}Ga]L1 radiolabeled with post-processed *n.c.a.* ^{68}Ga (III) [27] in sodium acetate buffer (pH 4, 98 °C, 15 min) were 80%–90%. After cartridge purification, the tracer showed a radiochemical purity (RCP) >98% as determined by radio-HPLC (Supporting Information, Fig. S1).



Scheme 1. Synthesis of DOTAGA(428-D-Lys)M^{BP} (L1): (i) dichloromethane (DCM), RT, 48 h, 74%. (ii) K₂CO₃, acetonitrile, 40 °C, 24 h, 51%. (iii) 1. H₂ (6 bar) Pd/C, MeOH, RT, 24 h. 2. H-D-Lys(Z)-OMe, DIPEA, HATU, dry DCM, RT, 12 h, 65% (iv) 1. H₂, Pd/C, MeOH, RT, 12 h. 2. 4-(*p*-iodophenyl)butyric acid, DIPEA, HATU, dry NMP, RT, 12 h, 73% (v) 1. TFA/DCM, RT, 12 h. 2. TMS-Br, dry DMF, RT, 12 h. 3. MeOH, RT, 12 h, 69%.

Table 1

Adsorption efficiency of ^{68}Ga -labeled ligands on hydroxyapatite (HA) after 10 min incubation (SD = standard deviation).

	^{68}Ga -BPAMD	^{68}Ga -L1	^{68}Ga -DOTA
% of activity on HA \pm SD	81.6 \pm 0.5	81.3 \pm 2.2	0.8 \pm 1.1

3.3. Adsorption on hydroxyapatite (HA)

Both ^{68}Ga -labeled bisphosphonate derivatives, ^{68}Ga -L1 and ^{68}Ga -BPAMD, showed an almost identical binding profile to hydroxyapatite (HA) after 10 min incubation time while ^{68}Ga -DOTA, as a control, showed no relevant adsorption on HA. The results are presented in Table 1.

3.4. Protein binding

Human serum protein binding was determined by ultrafiltration and indicated a significantly ($P < 0.005$) higher binding for ^{68}Ga -L1 compared to ^{68}Ga -BPAMD (Fig. 1). Binding of ^{68}Ga -L1 to human serum proteins was $88.1 \pm 5.9\%$ while that of ^{68}Ga -BPAMD was $28.8 \pm 1.1\%$. Retention of ^{68}Ga -L1 and ^{68}Ga -BPAMD on the ultrafilter in isotonic saline, in a control experiment, was $33.3 \pm 2.6\%$ and $15.0 \pm 1.7\%$, respectively.

3.5. Ex vivo organ distribution

Organ distribution of the ^{68}Ga -labeled compounds in selected tissues at 1 h, 3 h and 6 h p.i. in healthy male Wistar rats is presented in Supporting Information (Table S1). ^{68}Ga -BPAMD showed a fast blood clearance ($\%ID/g_{\text{blood}} = 0.25 \pm 0.04$) and a high degree of bone accumulation ($\%ID/g_{\text{femur}} = 2.24 \pm 0.42$) within 1 h, which is consistent to μPET results (see below), and matching the literature data [10]. ^{68}Ga -L1 showed an overall higher retention in the organism. Its radioactivity retention in soft tissue was higher already after 1 h p.i. which could be explained by a significant ($P < 0.001$) higher blood level of the albumin-binding bisphosphonate conjugate ($\%ID/g_{\text{blood}} = 2.01 \pm 0.18$). The accumulation of ^{68}Ga -L1 and ^{68}Ga -BPAMD in the skeleton was $36.4 \pm 10.0\%ID$ and $36.8 \pm 6.5\%ID$, respectively, indicating an almost identical ($P = 0.55$) accumulation on bone within 6 h. The ^{68}Ga -BPAMD activity in blood and in soft tissue organs decreased strongly over the examination time. Its blood level was significantly lower with a value of $0.3 \pm 0.1\%ID$ ($P < 0.001$) while its femur accumulation was comparable to that at 1 h ($P = 0.09$). Biodistribution of ^{68}Ga -L1 after 3 h p.i. showed only minor changes in soft tissue compared to that at 1 h values. In contrast, significant changes in the uptake profile were observed for blood ($P \leq 0.05$) and femur ($P < 0.05$). After 6 h p.i. femur accumulation of ^{68}Ga -L1 was found to be slightly higher than that at 3 h but showed no significance.

Table 2 shows the calculated total retention of ^{68}Ga -BPAMD and ^{68}Ga -L1 at 1 h, 3 h and 6 h p.i. in the blood and the skeleton. While the total

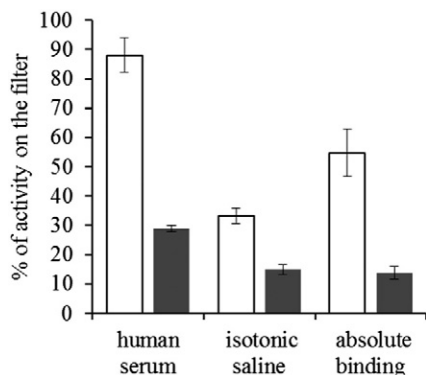


Fig. 1. Protein binding of ^{68}Ga -L1 (\square) and ^{68}Ga -BPAMD (\blacksquare) determined by ultrafiltration out of a triplicate. Low retention on the filter was observed for both tracers.

skeleton activity after 1 h, 3 h and 6 h showed no changes for ^{68}Ga -BPAMD, bone accumulation of ^{68}Ga -L1 increased over the time. Blood levels of ^{68}Ga -BPAMD dropped from $2.3 \pm 0.3\%ID$ (1 h) to $0.5 \pm 0.1\%ID$ (3 h) and to $0.3 \pm 0.1\%ID$ (6 h). After 6 h, $11.2 \pm 3.0\%ID$ of ^{68}Ga -L1 still remained in the blood pool. Fig. 2 presents results from the *ex vivo* organ distribution of ^{68}Ga -L1 over the whole examination time.

3.6. In vivo μPET

In vivo PET scans were conducted over 120 min p.i. for each ^{68}Ga -BPAMD and ^{68}Ga -L1 in one and the same animal. Images obtained after 120 min p.i. are consistent to the data obtained from *ex vivo* biodistribution experiments (see above). The skeleton is clearly visible in the ^{68}Ga -BPAMD PET scan with low background activity. ^{68}Ga -L1 showed bone uptake as well but with a distinctly higher background activity (Figs. 3 and 4). The higher background activity originates from the slower blood clearance of the albumin-binding bisphosphonate and is consistent to the results from *ex vivo* biodistribution (as above). Organs of high perfusion such as heart and abdominal aorta as well as branching to the common iliac arteries are well visible. No significant uptake in liver was observed for both radiotracers. The ^{68}Ga -L1 and ^{68}Ga -BPAMD were both excreted *via* the kidneys to the bladder. Particularly high accumulation of the radiotracers was found in the joint regions (Fig. 4) where bone metabolism is enhanced.

Time-activity curves (TAC) of the *in vivo* PET data are presented in Figs. 5 and 6. ^{68}Ga -BPAMD showed a fast uptake kinetics in the spine, reaching a plateau level between 35 and 40 min p.i. No significant changes in the SUV profile of the spine could be observed for the remaining scan time. The half-life of ^{68}Ga -BPAMD in the blood was $t_{1/2}(\alpha) = 6.5$ min. After 120 min, only marginal changes in the uptake profile were observed indicating that the body distribution and excretion had reached its kinetic completion. In contrast, no kinetic endpoint could be reached for the TAC of ^{68}Ga -L1 within 120 min scan time. The uptake profile of ^{68}Ga -L1 on the spine showed a delay in time. No plateau level was reached after 120 min and the accumulation rather followed a linear progression. Blood retention was obviously improved for ^{68}Ga -L1 with a half-life of $t_{1/2}(\alpha) = 37.8$ min (Table 3).

TAC of ^{68}Ga -BPAMD in the joint region between the femur and the tibia showed saturation profile (Fig. 7) and, in the spine region it reaches a higher plateau level after 120 min ($\text{SUV}_{\text{joint}} = 4.4$, $\text{SUV}_{\text{spine}} = 2.3$). The ratio in SUV between the joint of the femur and the tibia to the spine was 1.9 which reveals an almost doubled uptake of the radiotracer. TAC of ^{68}Ga -L1 in the joint region and in the spine (Figs. 6 and 7) showed a lower SUV compared to that of ^{68}Ga -BPAMD. After 120 min, the SUVs in the joint and the spine were 3.2 and 1.1, respectively. The graphs in Figs. 5 and 6 indicate no kinetic endpoint and, after 120 min, an SUV ratio of 2.9 between the femur and the tibia articulation and the spine was determined. This means an almost threefold higher uptake of ^{68}Ga -L1 at the high metabolic bone region compared to a twofold higher uptake of ^{68}Ga -BPAMD.

4. Discussion

^{177}Lu -BPAMD is an experimental therapeutic option for treatment of bone metastases [16]. However, its efficiency may be further improved as still more than half of injected dose is rapidly eliminated off the body. As bone uptake and renal elimination are rather swift, there are not too many options how to increase the dose delivered to the bone.

In this paper, we investigated the consequences of a chemical modification of the bisphosphonate BPAMD to delay its urinary excretion rate. The suggested modification of the BPAMD scaffold employs asymmetric substitution of *trans*-DO2A a glutaric acid and with acetamide-bis(phosphonate) pendant arm to give a DOTAGA-like BPAMD derivative. The new ligand, L1, is modified through the distant glutaric acid carboxylate group with an albumin-binding moiety. In this way, the charged coordinating acetate group is not lost due to formation of an

Table 2Bone and blood accumulation of ^{68}Ga -BPAMD and ^{68}Ga -L1 at 1 h, 3 h and 6 h p.i.

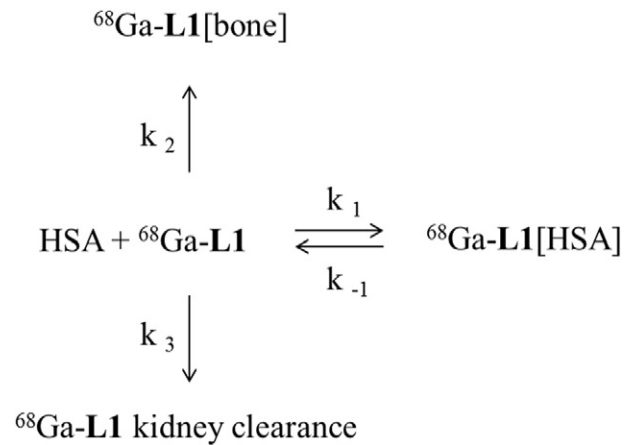
Organ	^{68}Ga -BPAMD			^{68}Ga -L1		
	1 h	3 h	6 h	1 h	3 h	6 h
Skeleton	36.3 ± 8.8	33.7 ± 3.4	36.8 ± 6.5	24.8 ± 3.8	32.1 ± 4.0	36.4 ± 10.0
Blood	2.3 ± 0.3	0.5 ± 0.1	0.3 ± 0.1	22.9 ± 2.1	17.2 ± 5.0	11.2 ± 3.0

Data are presented in mean % of injected dose ± SD of five animals (1 h, 3 h) and three animals (6 h).

additional amide bond which would lead to decrease of overall stability of the lutetium(III) complex. Since a potential therapy application with ^{177}Lu , as the long-term goal, was kept in mind, the preservation of seven donor groups together with a weakly coordinating amide moiety has been ensured. The chemical modification of BPAMD resulted in a compound, where both functionalities, the bisphosphonate and the albumin-binding moiety, are independently working in a single tracer.

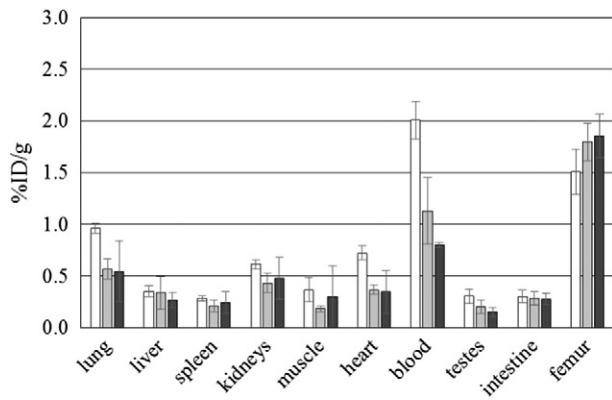
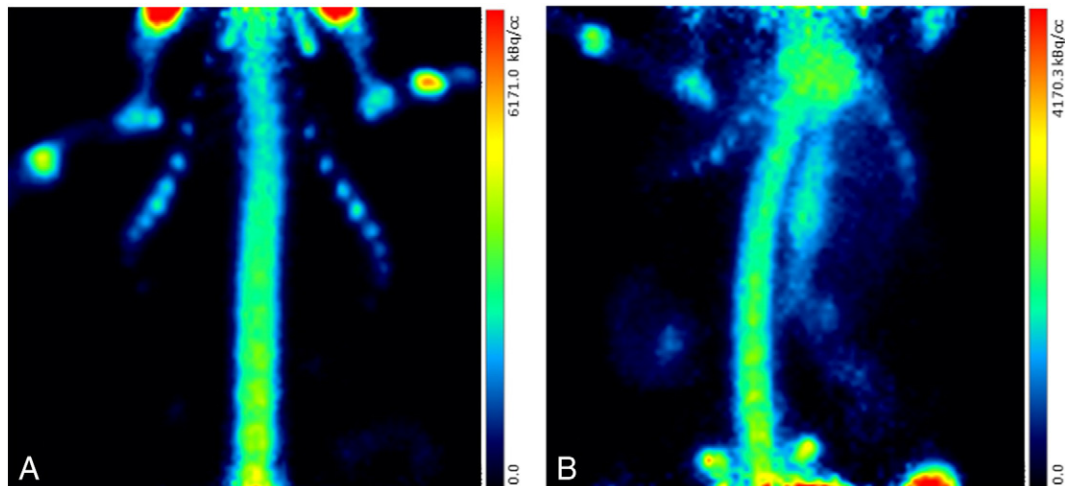
The new bifunctional compound showed a significant longer blood concentration over the investigated timescale in comparison to the non-modified bisphosphonate. Nevertheless, ^{68}Ga -L1 did not outclass ^{68}Ga -BPAMD in the total bone accumulation within 6 h, and uptake was close to be equal at these time points. The accumulation of ^{68}Ga -L1 in healthy bone depends on the adsorbing rate of the bisphosphonate on the calcified tissue and, on the other hand, depends on the bioavailability of the tracer. In the presence of albumin (35 to 53 g/L in human blood), a competition between binding to HSA and bone adsorption exists for ^{68}Ga -L1. It is to assume that the adsorption of bisphosphonates on the bone is nearly irreversible according to their long biological half-life in

the skeleton of several years [28], whereas the binding to HSA is relatively weak and reversible ($K_d = 3.3 \mu\text{M}$). As long as L1 is bound to HSA it cannot be excreted by the kidneys as well as adsorbed on the skeleton surface. The kinetics of ^{68}Ga -L1 *in vivo* is complex and difficult to estimate, since many compartments are involved, but it may be described by the following equation, whereby bone accumulation and kidney clearance are assumed as irreversible processes:



Future designs of bisphosphonates conjugated to an albumin binder moiety may include hydroxyl bisphosphonates, which are known to have a higher adsorption affinity to HAP [29] and thus may accelerate the skeletal accumulation (k_2) of the free ligand before it is cleared by the kidneys (k_3) or rebind to HSA (k_1). Alternatively, it is maybe useful to insert an albumin binder into the molecule of less strong binding to HSA.

We observed that the uptake ratio between the high-metabolic joint region and the ordinary bone was superior for the albumin binder conjugate (2.9 compared to 1.9). This might be a hint on how the tracers

**Fig. 2.** Ex vivo organ distribution ^{68}Ga -L1 at 1 h (□), 3 h (■) and 6 h (■) p.i.**Fig. 3.** Maximum intensity projection (MIP) of ^{68}Ga -BPAMD (A) and ^{68}Ga -L1 (B) at 2 h p.i. in healthy Wistar rats with the focus on the thorax region.

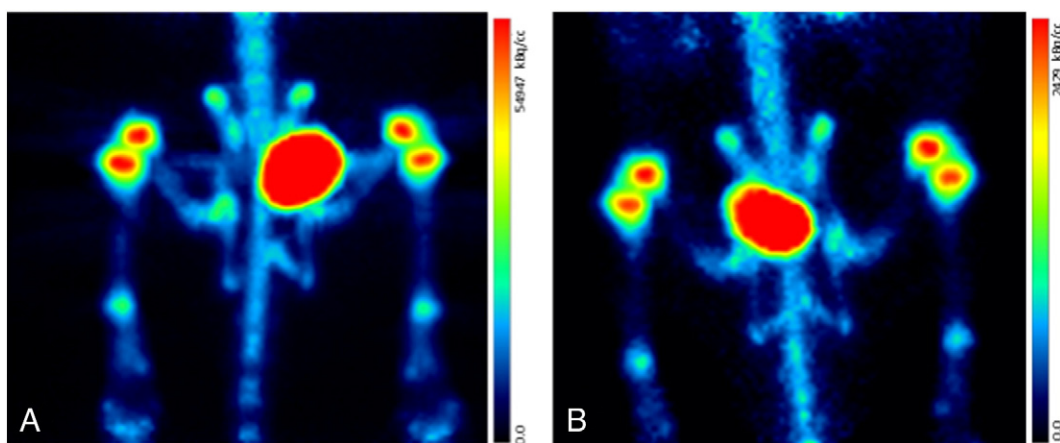


Fig. 4. Maximum intensity projection (MIP) of ^{68}Ga -BPAMD (A) and ^{68}Ga -L1 (B) at 2 h min p.i. in healthy Wistar rats with the focus on the pelvis region and the articulation between the femur and the tibia.

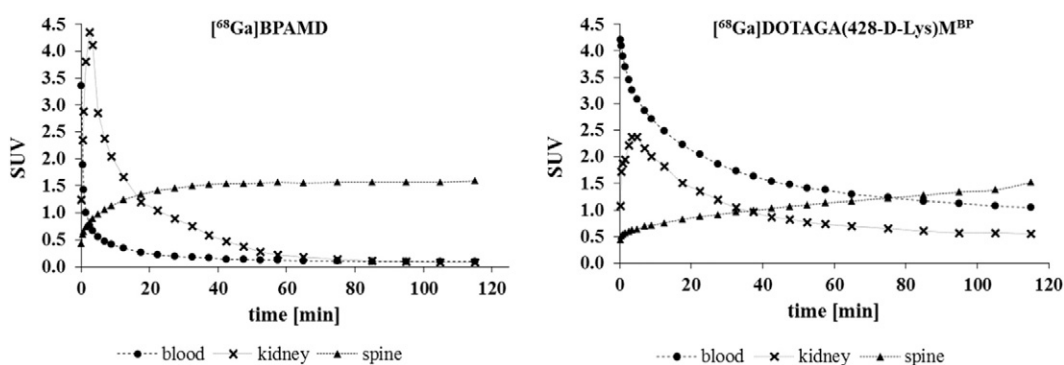


Fig. 5. Time-activity curves (TAC) determined over 2 h p.i. in selected tissues for ^{68}Ga -BPAMD and ^{68}Ga -L1 administered in one and the same animal.

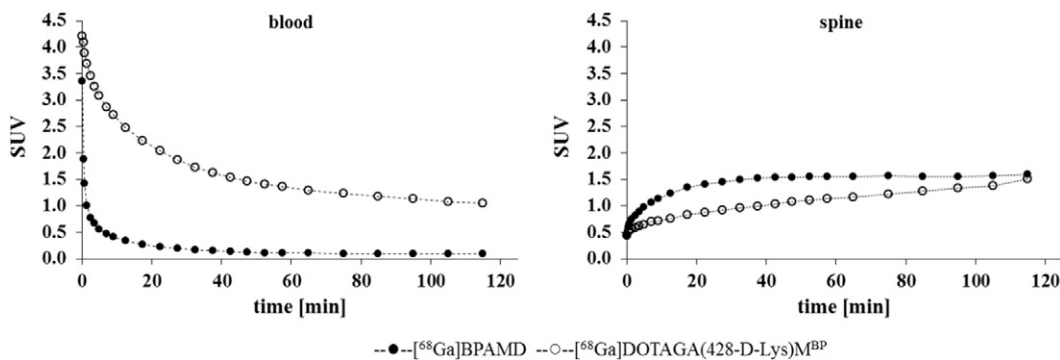


Fig. 6. Time-activity curves (TAC) determined over 2 h p.i. in the spine and the blood for ^{68}Ga -BPAMD and ^{68}Ga -L1 administered in one and the same animal.

would eventually perform when evaluated in a metastatic model or in patients expressing disseminated bone metastases. Tissue compartments with an enhanced turnover rate thus may benefit from compounds with a longer bioavailability. The consequences of the longer blood retention for a potential therapeutic application with ^{177}Lu are not yet evaluated but it is to assume that it is related to a higher dose delivered to the radiosensitive bone marrow. Strong accumulation in

tumor lesions in combination with high blood levels is likewise typical for antibodies used in radioimmunotherapy (RIT) with different radioisotopes, such as ^{131}I , ^{90}Y or ^{177}Lu . RIT showed promising results in oncology although it is related to moderate bone marrow toxicity [30]. Several antibodies are currently under evaluation all showing long-term blood retention [31,32], but as long as the uptake in tumor sites is convincingly high the potential toxicity is acceptable [33].

Table 3

Pharmacological parameters of the blood clearance of ^{68}Ga -BPAMD and ^{68}Ga -L1 determined from PET experiments in healthy Wistar rats.

Time	^{68}Ga -BPAMD	^{68}Ga -L1
$t_{1/2}(\alpha)$	6.5 min	37.8 min
$t_{1/2}(\beta)$	277 min	301 min

5. Conclusion

The chemical modification of BPAMD with the hydrophobic group leads to the DOTAGA-derived bisphosphonate macrocyclic chelate where the role of both functional groups, i.e., bone and HSA affinity, is independently preserved. The ^{68}Ga -L1 tracer shows significantly longer blood circulating time than ^{68}Ga -BPAMD and delayed whole body

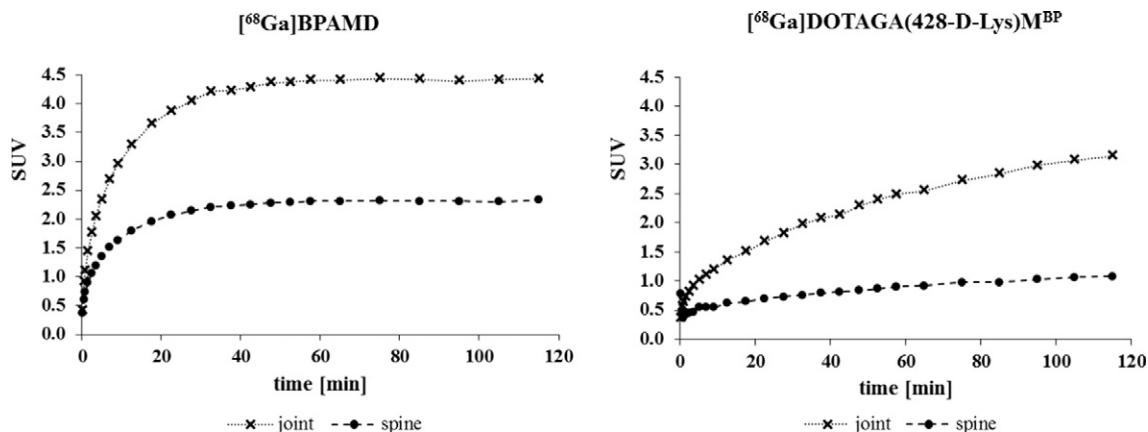


Fig. 7. Time-activity curves (TAC) determined over 2 h in the joint region between the femur and the tibia for ^{68}Ga -BPAMD and ^{68}Ga -L1 administered in one and the same animal.

clearance. In the small animal PET experiments with the ^{68}Ga tracers, the ratio between the high-metabolic joints and the ordinary bone was better for the albumin-binder conjugate compared to the non-modified parent compound. Overall bone accumulation became comparable already at 3 h p.i. As full pharmacokinetic equilibrium was not reached during time window available with the short-lived radioisotope, the delayed bone uptake should be more pronounced with radioisotopes of longer half-life.

This proof-of-principle study confirmed that utilizing reversible HSA binding of radiopharmaceuticals is a useful strategy to delay body elimination and to enhance the target accumulation. However, it was not our intention to apply the albumin-binder concept to a diagnostic ^{68}Ga -PET/CT bisphosphonate. In contrast, our intention was to understand the work in order to apply it to ^{177}Lu -labeled derivatives for treatment of disseminated bone metastases. Relating to a potential therapy with the ^{177}Lu -L1, comprehensive dosimetry studies are necessary to determine the consequences of the longer blood retention with regard to the whole body dose.

Conflict of interest

The authors declare that they have no conflict of interest.

Acknowledgment

This study was supported by grants from the Max Planck Graduate Center Main, the Wilhelm u. Ingeburg Dinse-Gedächtnis-Stiftung, Hamburg (provided to the THERANOSTICS Research Network, ENETS Center of Excellence, Zentralklinik Bad Berka, Germany) and the Grant Agency of the Czech Republic (13-08336S). We are grateful to Nicole Bausbacher and Barbara Biesalski for the animal handling. The networking support through the COST Action TD1004 is acknowledged.

Appendix A. Supplementary data

Supplementary data to this article can be found online at <http://dx.doi.org/10.1016/j.nucmedbio.2016.07.009>.

References

- Weilbaecher KN, Guise TA, McCauley LK. Cancer to bone: a fatal attraction. *Nat Rev Cancer* 2011;11:411–26.
- Rubini G, Nicoletti A, Rubini D, Asabella AN. Radiometabolic treatment of bone-metastasizing cancer: from (186)rhenium to (223)radium. *Cancer Biother Radiopharm* 2014;29:1–11.
- Paes FM, Serafini AN. Systemic metabolic radiopharmaceutical therapy in the treatment of metastatic bone pain. *Semin Nucl Med* 2010;40:89–104.
- Sartor O, Hoskin P, Bruland ØS. Targeted radio-nuclide therapy of skeletal metastases. *Cancer Treat Rev* 2013;39:18–26.
- Ogawa K, Kawashima H, Shiba K, Washiyama K, Yoshimoto M, Kiyono Y, et al. Development of [^{90}Y]DOTA-conjugated bisphosphonate for treatment of painful bone metastases. *Nucl Med Biol* 2009;36:129–35.
- Suzuji K, Satake M, Suwada J, Oshikiri S, Ashino H, Dozono H, et al. Synthesis and evaluation of a novel ^{68}Ga -chelate-conjugated bisphosphonate as a bone-seeking agent for PET imaging. *Nucl Med Biol* 2011;38:1011–8.
- Kubiček V, Rudovský J, Kotek J, Hermann P, vander Elst L, Müller RN, et al. A bisphosphonate monoamide analogue of DOTA: a potential agent for bone targeting. *J Am Chem Soc* 2005;127:16477–85.
- Fellner M, Riss P, Loktionova N, Zhernosekov K, Thews O, Gerdal CFGC, et al. Comparison of different phosphorus-containing ligands complexing ^{68}Ga for PET-imaging of bone metabolism. *Radiochim Acta* 2011;99:43–51.
- Vitha T, Kubiček V, Hermann P, vander Elst L, Müller RN, Kolar ZI, et al. Lanthanide(III) complexes of bis(phosphonate) monoamide analogues of DOTA: bone-seeking agents for imaging and therapy. *J Med Chem* 2008;51:677–83.
- Fellner M, Biesalski B, Bausbacher N, Kubiček V, Hermann P, Rösch F, et al. ^{68}Ga -BPAMD: PET-imaging of bone metastases with a generator based positron emitter. *Nucl Med Biol* 2012;39:993–9.
- Meckel M, Fellner M, Bergmann R, Rösch F. *In vivo* comparison of DOTA based ^{68}Ga -labelled bisphosphonates for bone imaging in non-tumour models. *Nucl Med Biol* 2013;40:823–30.
- Fellner M, Baum RP, Kubiček V, Hermann P, Lukeš I, Prasad V, et al. PET/CT imaging of osteoblastic bone metastasis with ^{68}Ga -bisphosphonates: first human study. *Eur J Nucl Med Mol Imaging* 2010;37:834.
- Rösch F, Baum RP. Generator-based PET radiopharmaceuticals for molecular imaging of tumours: on the way to theranostics. *Dalton Trans* 2011;40:6104–11.
- Yousefnia H, Zolghadri S, Shanehsazzadeh S. Estimated human absorbed dose of ^{177}Lu -BPAMD based on mice data: comparison with ^{177}Lu -EDTMP. *Appl Radiat Isot* 2014;104:128–35.
- Bergmann R, Meckel M, Kubiček V, Pietzsch J, Steinbach J, Hermann P, et al. ^{177}Lu -labelled macrocyclic bisphosphonates for targeting bone metastasis in cancer treatment. *EJNMMI Res* 2016;6:5.
- Baum RP, Kulkarni HR. Theranostics: From molecular imaging using ^{68}Ga labeled tracers and PET/CT to personalized radionuclide therapy—the Bad Berka experience. *Theranostics* 2012;2:437–47.
- Meckel M, Nauth A, Timpe J, Zhernosekov K, Puranik AD, Baum RP, et al. Development of a [^{177}Lu]BPAMD labeling kit and an automated synthesis module for routine bone targeted endoradiotherapy. *Cancer Biother Radiopharm* 2015;30:94–9.
- Bartl R, Frisch B, von Tresckow E, Bartl C. Bisphosphonates in medical practice. Berlin Heidelberg: Springer-Verlag; 2007 43–6.
- Merbach A, Helm L, Tóth E. The chemistry of contrast agents in medical magnetic resonance imaging. 2nd ed. Hoboken: Wiley; 2013.
- Dumelin CE, Trüssel S, Buller F, Trachsel E, Neri D, Scheuermann J. A portable albumin binder from a DNA-encoded chemical library. *Angew Chem Int Ed* 2008;47:3196–201.
- Fani M, Wang X, Nicolas G, Medina C, Raynal I, Port M, et al. Development of new folate-based PET radiotracers: preclinical evaluation of ^{68}Ga -DOTA-folate conjugates. *Eur J Nucl Med Mol Imaging* 2011;38:108–19.
- Müller C, Struthers H, Winiger C, Zhernosekov K, Schibli R. DOTA conjugate with an albumin-binding entity enables the first folic acid-targeted ^{177}Lu -radionuclide tumor therapy in mice. *J Nucl Med* 2013;54:124–31.
- Fischer CR, Groehn V, Reber J, Schibli R, Ametamey SM, Müller C. Improved PET imaging of tumors in mice using a novel ^{18}F -folate conjugate with an albumin-binding entity. *Mol Imaging Biol* 2013;15:649–54.
- Riss PJ, Burchardt C, Rösch F. A methodical ^{68}Ga -labelling study of DO2A-(butyl-L-tyrosine)₂ with cation-exchanger post-processed ^{68}Ga : practical aspects of radiolabelling. *Contrast Media Mol Imaging* 2011;6:492–8.
- Eisenwiener KP, Powell P, Maecke HR. A convenient synthesis of novel bifunctional prochelators for coupling to bioactive peptides for radiometal labelling. *Bioorg Med Chem Lett* 2000;10:2133–5.
- Lee HB, Blafox MD. Blood volume in the rat. *J Nucl Med* 1985;26:72–6.

- [27] Zhernosekov K, Filosofov DV, Baum RP, Aschoff P, Bihl H, Razbash AA, et al. Processing of generator-produced ^{68}Ga for medical application. *J Nucl Med* 2007;48:1741.
- [28] Lin JH. Bisphosphonates: a review of their pharmacokinetic properties. *Bone* 1996;18:75–85.
- [29] Nancollas GH, Tang R, Phipps RJ, Henneman Z, Gulde S, Wu W, et al. Novel insights into actions of bisphosphonates on bone: differences in interactions with hydroxyapatite. *Bone* 2006;38:617–27.
- [30] Tagawa ST, Milowsky MI, Morris M, Vallabhajosula S, Christos P, Akhtar NH, et al. Phase II study of lutetium-177-labeled anti-prostate-specific membrane antigen monoclonal antibody J591 for metastatic castration-resistant prostate cancer. *Clin Cancer Res* 2013;19:5182–91.
- [31] Tagawa ST, Beltran H, Vallabhajosula S, Goldsmith SJ, Osborne J, Matulich D, et al. Anti-prostate specific membrane antigen-based radioimmunotherapy for prostate cancer. *Cancer* 2010;116:1075–83.
- [32] Ray GL, Baidoo KW, Keller LMM, Albert PS, Brechbiel MW, Milenic DE. Pre-clinical assessment of ^{177}Lu -labeled trastuzumab targeting HER2 for treatment and management of cancer patients with disseminated intraperitoneal disease. *Pharmaceuticals* 2012;5:1–15.
- [33] Wiseman GA, White CA, Sparks RB, Erwin WD, Podoloff DA, Lamonica D, et al. Biodistribution and dosimetry results from a phase III prospectively randomized controlled trial of Zevalin radioimmunotherapy for low-grade, follicular, or transformed B-cell non-Hodgkin's lymphoma. *Crit Rev Oncol Hematol* 2001;39:181–94.